Comparative Performance in Load Frequency Stabilization by Coordinated Control with SMES and without SMES for a Bilateral Two area Thermal – Thermal System

Himanshi Singla
Dept. of electrical engineering
NIT Kurukshetra
Kurukshetra
E-mail:singla.himanshi1@gmail.com

Ashwini Kumar
Dept. of electrical engineering
NIT Kurukshetra
Kurukshetra
E-mail:ashwa_ks@yahoo.co.in

Abstract: *This paper presents the analysis of automatic generation control (AGC) of an interconnected bilateral two area thermal- thermal system. As an interconnected power system has large number of area frequency oscillation. To compensate these oscillations, the additions of small capacity super conducting magnetic energy storage (SMES) unit in area 1 or 2 are studied. The optimal values of the integral gain settings are obtained by using the linear quadratic regulator. Analysis reveals that SMES unit is fitted in either area improves the dynamic performance to a considerable extent following a load disturbance in either of area. The results obtained by using LQR and compared by with or without SMES.*

Keywords - AGC; SMES; LQR; LFC; ACE; GENCO; DISCO; TRANSCO.

I. Nomenclature

T_{P1} , T_{P2}	power system time constants,
$K_{P1,}$ K_{P2}	power system gains,
T_T	turbine time constant,
T_G	governor time constant of thermal area,
T_w	water time constant,
ΔF	Incremental Frequency,
$R_{1,}$ R_2	governor speed regulation parameters of thermal areas.
$P_{R1,}$ P_{R2}	rated area capacities (a12=P_{R1} /P_{R2}).
T_{12}	synchronizing coefficient
B	frequency bias constant
K_I	Integral Gain Constant.
K_{SMES}	gain for SMES
T_{SMES}	time constant for SMES
apf	area participation factor
K_f	frequency gain

II. Introduction

In power systems, changes in the load, affect the frequency and bus voltages in the systems. For small changes in the load the frequency deviation problem can be separated or decoupled from the voltage deviation. The problem of controlling the real power output of generating units in response to changes in system frequency and tie-line power interchange within specified limits is known as load frequency control (LFC). It is generally regarded as a part of automatic generation control (AGC) and is very important in the operation of power systems [1].With the increase in size and complexity of modern power systems, inadequate control may deteriorate the frequency and system oscillation might propagate into wide area resulting in a system blackout. However, most of the solutions proposed so far for AGC have not been implemented due to system operational constraints associated with thermal power plants. The main reason is the non-availability of required stored energy capacity other than the inertia of the generator rotors. Fast-acting energy storage system provides storage capacity in addition to the kinetic energy of the generator rotors which can share sudden changes in power requirement and effectively damp electromechanical oscillations in a power system. A superconducting magnetic energy storage (SMES) which is capable of controlling active and reactive powers simultaneously [2] is expected as one of the most effective and significant stabilizer of frequency oscillations. The viability of superconducting magnetic energy storage (SMES) for power system dynamic performance improvement has been reported.

Identify applicable sponsor/s here. If no sponsors, delete this text box. (sponsors)

For studying and improvement of the performances of all Controllers various optimization algorithms and techniques have resorted. But a more recent and powerful computational intelligence technique linear quadratic regulator to optimize the PI gains of the controller.

Identify applicable sponsor/s here. If no sponsors, delete this text box. (sponsors)

III. SMES System

The schematic diagram in fig.1 shows the configuration of a thyristor controlled SMES unit [3-5]. The SMES unit contains DC superconducting coil and converter which are connected by Y–Δ/Y–Y transformer. The control of the converter firing angle provides the dc voltage Ed appearing across the inductor to be continuously varying within a certain range of positive and negative values. The inductor is initially charged to its rated current Id0 by applying a small positive voltage. Once the current reaches the rated value, it is maintained constant by reducing the voltage across the inductor to zero since the coil is superconducting [5]. Neglecting the transformer and the converter losses, the DC voltage is given by

$$E_d = 2\ Vd_0\ \cos\alpha - 2I_dR_c \quad (1)$$

Where E_d is DC voltage applied to the inductor (kV), α is firing angle (^{0}), I_d is current flowing through the inductor (kA). R_c is equivalent commutating resistance (Ω) and Vd_0 is maximum circuit bridge voltage (kV). Charge and discharge of SMES unit are controlled through change of commutation angle α. If α is less than 90^0, converter acts in converter mode and if α is greater than 90^0, the converter acts in an inverter mode (discharging mode). In AGC operation, the dc voltage Ed across the superconducting inductor is continuously controlled depending on the sensed area control error (ACE) signal. In literatures, it is taken to be dependent on the sensed Δf signal or ACE defined as Bi Δfi + αPi (i = 1… 3)[6].

The expression of ΔPi is given and Bi parameters are chosen as 1/Kpi + 1/R_i. In this study, as in recent literature, inductor voltage deviation of SMES unit of each area is based on ACE of the same area in power system [7]. Moreover, the inductor current deviation is used as a negative feedback signal in the SMES control loop. So, the current variable of SMES unit is intended to be settling to its steady state value. If the load demand

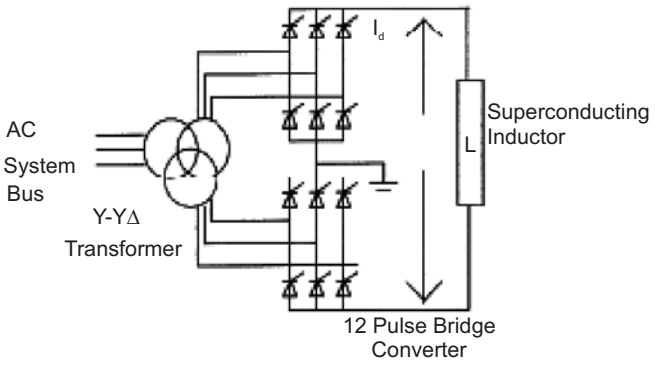

Fig. 1 Schematic diagram of SMES unit

changes suddenly, the feedback provides the prompt restoration of current. The inductor current must be restored to its nominal value quickly after a system disturbance, so that it can respond to the next load disturbance immediately[3-5]. The incremental change in the voltage applied to the inductor is expressed as

$$\Delta E_d = \left[\frac{K_{SMES}}{1+sT_{Dc}}\right]\Delta Error_1 \quad (2)$$

Where, ΔEd is the incremental change in converter voltage, T_{DC} is the converter time delay, K_{SMES} is the gain of the control loop and ΔError is the input signal to the SMES control logic. The inductor current deviation is given by

$$\Delta Id = \Delta Ed\ /sL \quad (3)$$

In this work, area control error (ACE) of area 1 is considered as the input signal to the SMES control logic (i.e., "Error1 = ACE1). The area control error of the two areas are defined as

$$ACEi = Bi\Delta fi + \Delta Ptieij; \qquad i, j = 1, 2, \quad (4)$$

Where Δfi is the change in frequency of area i and ΔPij is the Change in tie-line power flow out of area i–j. Thus, from Eqs. (2) and (4),

All the SMES data is given in Appendix A. As a result, the equations of inductor voltage deviation and current deviation for each area in Laplace domain are as follows

$$\Delta E_d = \frac{K_{SMES}}{1+sT_{DC}}\left(B_1\Delta f_1 + \Delta P_{tie12}\right) \quad (5)$$

Note that ΔError1 = ACE1 = (B1Δ f1 + $\Delta Ptie_{12}$). However, it is reported in [8-10] that, the inductor current in the SMES unit will return to its nominal value very slowly only if Eq. (5) is used. But, the inductor current must be restored to its nominal value quickly after a system disturbance so that it can respond to the next load perturbation immediately. Hence, the inductor

current deviation can be sensed and used as a negative feedback signal in the SMES control loop so that the current restoration to its nominal value can be enhanced. The block diagram representation of SMES incorporating the negative inductor current deviation feedback is shown in Fig. 2. Thus the dynamic equations for the inductor voltage deviation and current deviation of the SMES unit area

$$\Delta E_d = \frac{1}{1+sT_{DC}}[K_{SMES}(B_1\Delta f_1 + \Delta P_{tie12}) - K_{id}\,\Delta I_d] \qquad (6)$$

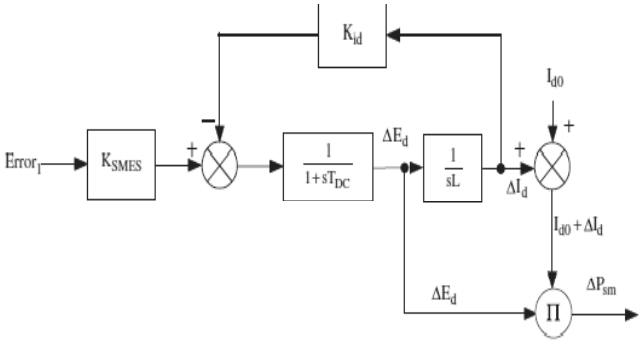

Fig.2 SMES block diagram with negative inductor current deviation feedback

.

III. Modelling for Automatic Generation Control of the Power System with Two Areas

The model of a two-area power system suitable for a digital simulation of AGC is developed for the analysis as shown in Fig. 3. Two areas are connected by a weak tie-line. When there is sudden rise in power demand in one area, the stored energy is almost immediately released by the SMES through its power conversion system. As the governor control mechanism starts working to set the power system to the new equilibrium condition, the SMES coil stores energy back to its nominal level. Similar is the action when there is a sudden decrease in load demand. Basically, Fig. 3. Typical Simulation Model of Two-Area System the operation speed of governor-turbine system is slow compared with that of the excitation system. As a result, fluctuations in terminal voltage can be corrected by the excitation system very quickly, but fluctuations in generated power or frequency are corrected slowly since load frequency control is primarily concerned with the real power/frequency behavior, the excitation system model will not be required in the analysis[8]. The modeling and control design aspects of SMES are separately described in detail.

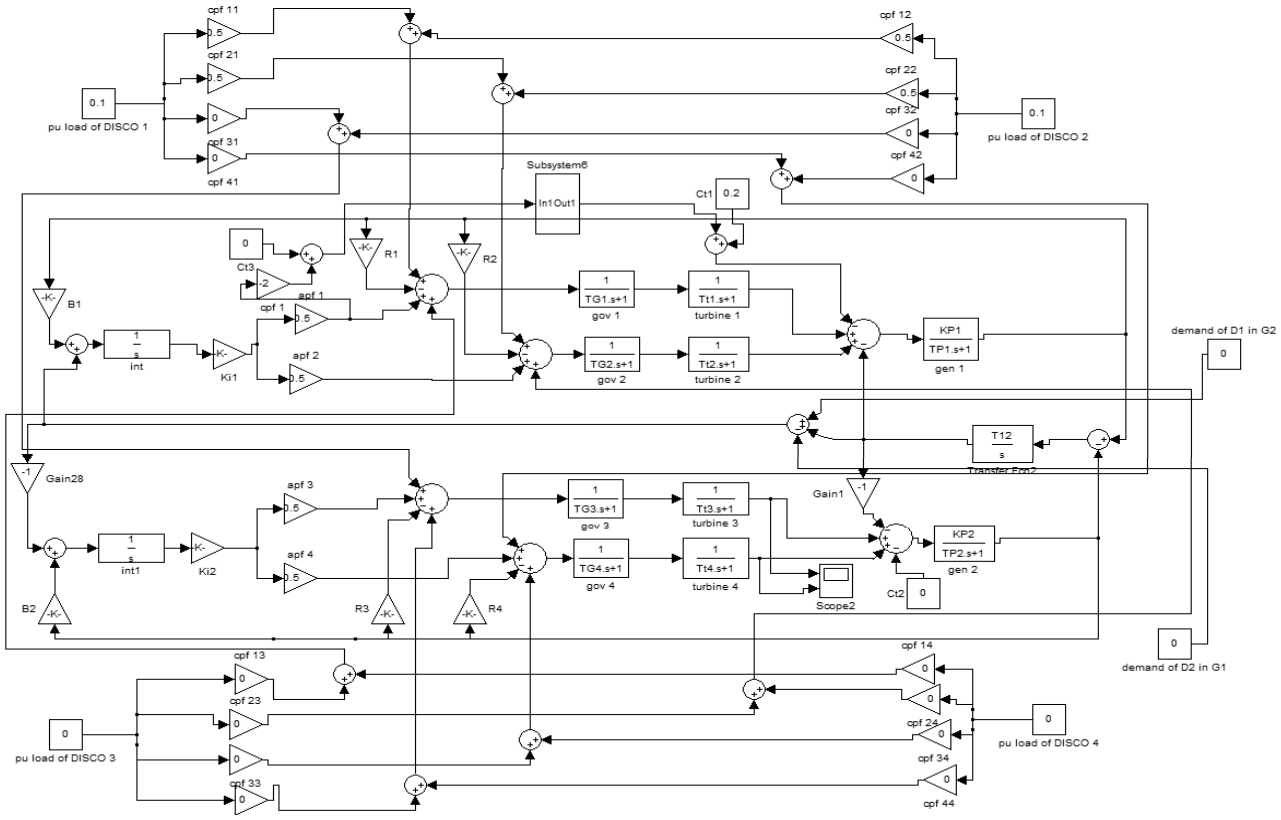

Fig. 3 Linearised model of interconnected two area thermal-thermal restructured power system

A. Restructured system

The traditional power system industry has a "vertically integrated utility" (VIU) structure. In the restructured or deregulated environment, vertically integrated utilities no longer exist. The utilities no longer own generation, transmission, and distribution; instead, there are three different entities, GENCOs (generation companies), TRANSCOs (transmission companies) and DISCOs (distribution companies). As there are several GENCOs and DISCOs in the deregulated structure, a DISCO has the freedom to have a contract with any GENCO for transaction of power. A DISCO may have a contract with a GENCO in another control area. Such transactions are called "bilateral transactions." All the transactions have to be cleared through an impartial entity called an independent system operator (ISO). The ISO has to control a number of so-called "ancillary services," one of which is AGC.

B. DISCO Participation Matrix

In the restructured environment, GENCOs sell power to various DISCOs at competitive prices. Thus, DISCOs have the liberty to choose the GENCOs for contracts. They may or may not have contracts with the GENCOs in their own area. This makes various combinations of GENCO-DISCO contracts possible in practice. We introduce the concept of a "DISCO participation matrix" (DPM) to make the visualization of contracts easier. DPM is a matrix with the number of rows equal to the number of GENCOs and the number of columns equal to the number of DISCOs in the system. Each entry in this matrix can be thought of as a fraction of a total load contracted by a DISCO (column) toward a GENCO (row). Thus, the ith entry corresponds to the fraction of the total load power contracted by DISCO from a GENCO. The sum of all the entries in a column in this matrix is unity. DPM shows the participation of a DISCO in a contract with a GENCO, hence the name "DISCO participation matrix." Consider a two-area system in which each area has two GENCOs and two DISCOs in it. Let GENCO1, GENCO2, DISCO1, and DISCO2 be in area I and GENCO3, GENCO4, DISCO3, and DISCO4 be in area II as shown in Fig. 1.

C. Base Case

Consider a case where the GENCOs in each area participate equally in AGC; i.e., ACE participation factors are apf1=0.5, apf2=1-0.5, apf3 =0.5, apf4 = 1- 0.5. Assume that the load change occurs only in area I. Thus, the load is demanded only by DISCO and DISCO. Let the value of this load demand be 0.1 pu MW for each of them. Note that DISCO do not demand power from any GENCOs, and hence the corresponding participation factors are zero. DISCO1 and DISCO2 demand identically from their local GENCOs, like GENCO1 and GENCO2. Fig. 4 shows the results of this load change: area frequency deviations, actual power flow on the tie line (in a direction from area I to area II), and the generated powers of various GENCOs, following a step change in the load demands of DISCO1 and DISCO2. The frequency deviation in each area goes to zero in the steady state. Since the off diagonal blocks of DPM are zero, i.e., there are no contracts of power between a GENCO in one area and a DISCO in another area, the scheduled steady state power flow over the tie line is zero. The actual power on the tie line goes to zero. In the steady state, generation of a GENCO must match the demand of the DISCOs in contract with it. This desired generation of a GENCO in pu MW can be expressed in terms of cpf's and the total demand of DISCOs as Referring

$$\Delta P_{Mi} = \sum_j cpf_{ij}\, \Delta P_{Lj} \qquad (7)$$

Where ΔP_{Lj} is the total demand of DISCO j and cpf_{ij} are given *by DPM. In the two-area case,*

$$\Delta P_{Mi=} cpf_{i1}\Delta P_{L1} + cpf_{i2}\Delta P_{L2} + cpf_{i3}\Delta P_{L3} + cpf_{i4}\Delta P_{L4}$$

For the case under consideration, we have,

$$\Delta P_{M1} = 0.5 * \Delta P_{L1} + 0.5 * \Delta P_{L2} = 0.1 pu\ MW$$

Similarly:

$$\Delta P_{M2} = 0.1\ pu\ MW$$
$$\Delta P_{M3} = 0\ pu\ MW$$
$$\Delta P_{M4} = 0 pu\ MW$$

IV. Optimal Controller or AGC After Deregulation

Optimal control [10, 11] is the branch of optimal control theory that deals with designing for dynamic system by minimizing a performance index that depends on the system variables. The design of optimal controllers for linear systems with quadratic performance index is called linear quadratic regulator (LQR) problem. The objective if the regulator design is to determine the optimal control law u^* (x, t) which can transfer the system from its initial state to final state such that a given performance index is minimized. The performance index is selected to give the best tradeoff between performance and cost of control. The performance index

that is widely used in optimal control design is known as the quadratic performance index and is based on minimum error and minimum energy criteria.

Modern control theory is applied in this section to design an optimal load frequency controller for a two area system. In accordance with modern control terminology "ΔP_{c1}, ΔP_{c2}" will be reffered to as control inputs u_1 and u_2 were provided by the integral of ACE_s. In modern control theory approach u_1 and u_2 will be created by a linear combination of all the system states. For formulating the state variable model for this purpose the conventional feedback loops are opened and each time constant is represented by a separate block as shown in figure. State variables are defined as the outputs of all blocks having either an integrator or a time constant. We immediately notice that the system has thirteen state variables. Before presenting the optimal design, we must formulate the state model. This is achieved below by writing the differential equations describing each individual block in terms of state variables.

For block **1**

$$\dot{x_1} = \frac{-1}{T_{Ps1}}x1 + \frac{K_{Ps1}}{T_{Ps1}}x2 + \frac{K_{Ps1}}{T_{Ps1}}x4 - \frac{K_{Ps1}}{T_{Ps1}}x13 - \frac{K_{Ps1}}{T_{Ps1}}\omega 1 \quad (9)$$

For block **2**

$$\dot{x_2} = \frac{-1}{T_{t1}}x2 + \frac{1}{T_{t1}}x3 \quad (10)$$

For block **3**

$$\dot{x_3} = \frac{-1}{R_1 T_{sg1}}x1 - \frac{1}{T_{sg1}}x3 + \frac{apf_1}{T_{sg1}}u_1 \quad (11)$$

For block **4**

$$\dot{x_4} = \frac{-1}{T_{t2}}x4 + \frac{1}{T_{t2}}x5 \quad (12)$$

For block **5**

$$\dot{x_5} = \frac{-1}{R_2 T_{sg2}}x1 - \frac{1}{T_{sg2}} + \frac{apf_2}{T_{sg2}}u_1 \quad (13)$$

For block **6**

$$\dot{x_6} = \frac{-1}{T_{Ps2}}x6 + \frac{K_{Ps2}}{T_{Ps2}}x7 + \frac{K_{Ps2}}{T_{Ps2}}x9 - \frac{a_{12}K_{Ps2}}{T_{Ps2}}x13 \quad (14)$$

For block **7**

$$\dot{x_7} = \frac{-1}{T_{t3}}x7 + \frac{1}{T_{t3}}x8 \quad (15)$$

For block **8**

$$\dot{x_8} = \frac{-1}{R_3 T_{sg3}}x6 - \frac{1}{T_{sg3}}x8 + \frac{apf_3}{T_{sg3}}u_2 \quad (16)$$

For block **9**

$$\dot{x_9} = \frac{-1}{T_{t4}}x9 + \frac{1}{T_{t4}}x10 \quad (17)$$

For block **10**

$$\dot{x_{10}} = \frac{-1}{R_4 T_{sg4}}x6 - \frac{1}{T_{sg4}}x10 + \frac{apf_4}{T_{sg4}}u_2 \quad (18)$$

For block **11**

$$\dot{x_{11}} = B_1 x1 + x13 \quad (19)$$

For block **12**

$$\dot{x_{12}} = B_2 x6 + a_{12}x13 \quad (20)$$

For block **13**

$$\dot{x_{13}} = 2\pi T_{12}x1 - 2\pi T_{12}x6 \quad (21)$$

The thirteen equations (8) – (21) can be recognized in the following vector matrix form

$$\dot{x} = Ax + Bu + Fw \quad (22)$$

$x=[x1\ x2\ .....]^T$ state vector

$u= [u_1\ u_2\ .....]$ control vector

In the conventional control scheme u_1 and u_2 are constructed as under from the state variables x_{11} and x_{12} only.

$u_1 = -K_{i1}\ x11 = -K_{i1} \int ACE_1\, dt$

$u_2 = -K_{i2}\ x12 = -K_{i2} \int ACE_2\, dt$

In the optimal control theory the control inputs u_1 and u_2 are generated by means of feedback from all the states with feedback constants to be determined with an optimality criterion. All the values of system variables are given in Appendix A.

Examination of equation (22) reveals that the model is not in the standard form employed in optimal control theory. The standard form is

$$\dot{x} = Ax + Bu$$

Which does not contain the disturbance term Fw present in eq. (21). Further, a constant disturbance vector ***w*** would derive some of the system states and the control vector ***u*** to constant steady values. While cost function employed in optimal control requires that the system state and control vectors have zero steady state value for the cost function to have a minimum.

For a constant disturbance vectors w, the steady state is reached when

$$\dot{x} = 0$$

In eq. (21); Which then gives,

$$0 = Ax_{ss} + Bu_{ss} + Fw$$

Defining ***x*** and ***u*** as the sum of transient and steady state terms, we can write

$$x = \acute{x} + x_{ss} \quad (23)$$
$$u = \acute{u} + \acute{u}_{ss} \quad (24)$$

Substituting $\boldsymbol{x}$ and $\boldsymbol{u}$ from above equations, we have

$$\dot{x}_{ss} + \dot{x}' = A(x' + x_{ss}) + B(u' + u_{ss}) + Dp + Fw$$

By virtue of relationship, we get

$$\acute{x} = A\acute{x} + Bu$$

This represents system model in terms of excursion of state and control vectors from their respective steady state values.

For full state feedback, the control vector $\boldsymbol{u}$ is constructed by a linear combination of all states, i.e.

$$u = -Kx$$

Where $\boldsymbol{K}$ is the feedback matrix.

Now

$$\acute{u} + u_{ss} = -K(\acute{x} + x_{ss})$$

For a stable system both $\boldsymbol{x'}$ and $\boldsymbol{u'}$ go to zero, therefore

$$u_{ss} = -Kx_{ss}$$

Hence the feedback matrix **K** in eqn. is to be determined so that a certain performance index (PI) is minimized in transferring the system state from an arbitrary initial state $\boldsymbol{x'(0)}$ to origin in infinite time (i.e. $\boldsymbol{x'(\infty) = 0}$).

A convenient PI has the quadratic form

$$\boldsymbol{PI} = \frac{1}{2}\int_0^\infty (\boldsymbol{x'^T Q x' + u'^T R u'})dt$$

The matrix $\boldsymbol{Q}$ and $\boldsymbol{R}$ are defined for the problem using following the design considerations:

(i) Excursions of ACEs about the steady values ($x'_{13} + B_1 x'_1$; $-a_{12} x'_{13} + B_2 x'_6$) are minimized. The Steady state values of ACEs are ofcourse zero.

(ii) Excursions of $\int$ ACE dt about the steady state value are(x'_{11}, x'_{12}) minimized. The steady state values of $\int$ ACE dt are, of course, constants.

(iii) Excursions of control vector ($\boldsymbol{u_1}$, $\boldsymbol{u_2}$) about the Steady value are minimized. The steady value of the control vector is, of course, a constant. This minimization is intended to indirectly limit the control effort within the physical capability of components.

With the above reasoning, we can write the PI as

$$PI = \int_0^\infty [(\acute{x}_{13} + B_1\acute{x}_1)^2 + (a_{12}\acute{x}_{13} + B_2\acute{x}_6)^2 + (\acute{x}_{11}^2 + \acute{x}_{12}^2) + K(\acute{u}_1^2 + \acute{u}_2^2)] \quad (25)$$

R= KI = symmetric matrix

Determination of feedback matrix K which minimizes the above PI is the standard optimal regulator problem.

The acceptable solution of K is that for which the system remains stable. For stability all the Eigen values of the matrix (A - BK) should have negative real parts.

V. Results and Discussion

Simulation studies are performed to investigate the per-formance of the bilateral two-area thermal-thermal system without and with SMES unit in area 1 considering LQR. A step load disturbance of the nominal loading is considered in area 1. It is observed that after the load disturbance, the area frequency response is heavily perturbed. Hence, to suppress the oscillations and to have the optimal transient response of area frequencies and tie line power exchange, the impacts of SMES in area 1 have been explored and discussed as below.Fig.4 gives the dynamic responses like frequency deviations and inter-area tie-power oscillations with some step load disturbance in the thermal area without SMES as well as, with an SMES unit in area 1. It can be observed that, the transient behavior of area frequencies and tie-power have improved significantly in terms of peak deviations and settling time in the presence of the SMES unit.

The transient responses for the systems shown in Fig. 3 with SMES are depicted in Fig. 4(b) after load perturbation in Area 1. The results clearly indicate that the coordination of SMES can be effectively employed to dynamically stabilize the multiple-units thermal-thermal system and suppress the oscillations in area frequencies and the tie-line power exchange under load disturbance. The gains of the integral controller are optimized individually through LQR optimization algorithms for all parameter-sets. The results for a few sets of SMES and without SMES are given in Table 1. The undershoot (US), overshoot (OS) and settling time (ts) of area frequencies and tie-line power are presented. SMES placed in area 1 gives minimum undershoot and overshoot in frequency oscillations as well as tie-line power exchange as compared to without SMES. However, without SMES the oscillations in frequency of Area 1 and tie-line power take longer time to settle. On the other hand, when SMES is placed it is very effective to quickly suppress the oscillations in area frequencies and tie-line power. Fig. 5 shows the comparison of with or without SMES obtained by LQR algorithm.

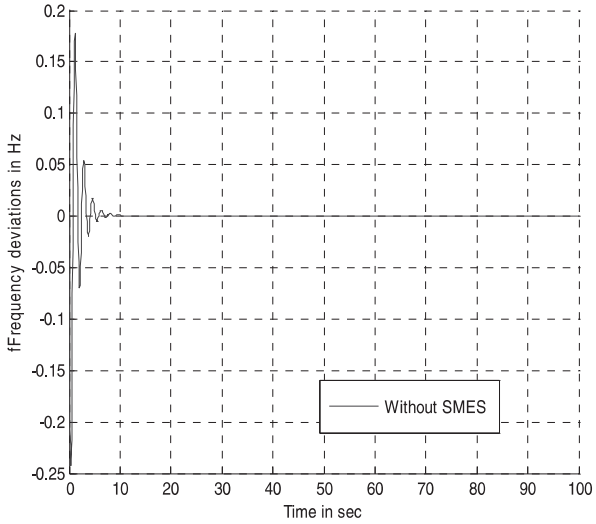

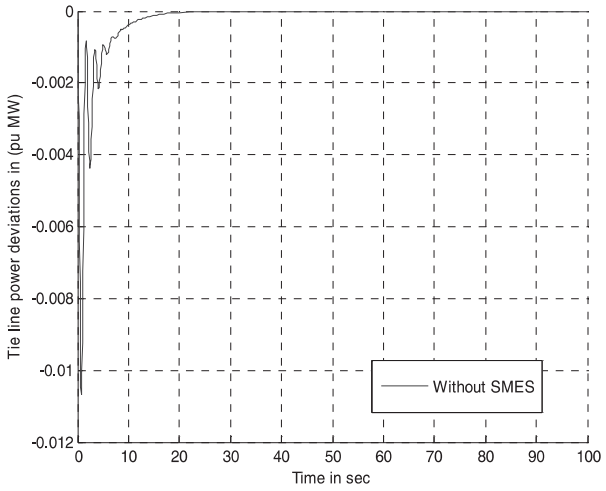

Fig.4 (a) Frequency deviation and tie line power deviation in area 1 without SMES

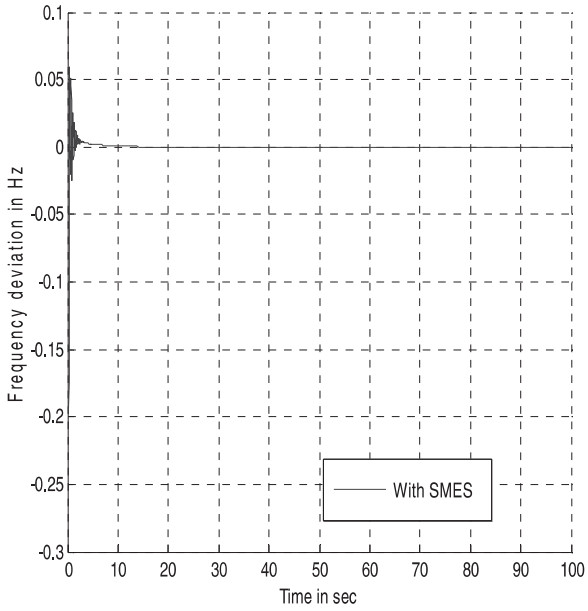

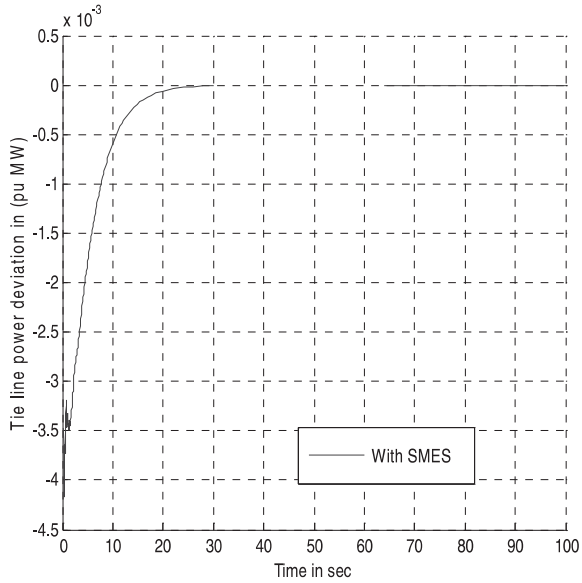

Fig.4 (b) Frequency deviation and tie line power deviation in area 1 with SMES

Table 1 Results for dynamic responses with or without SMES

Sr. No.			Without SMES	With SMES
1.	Δf_1	Us,Os, Ts	0.22, 0.17, 10	0.17, 0.06, 7
2.	ΔP_{tie}	Us,Os, Ts	0.010, 0.0021, 20	0.0035, 0.0005, 19

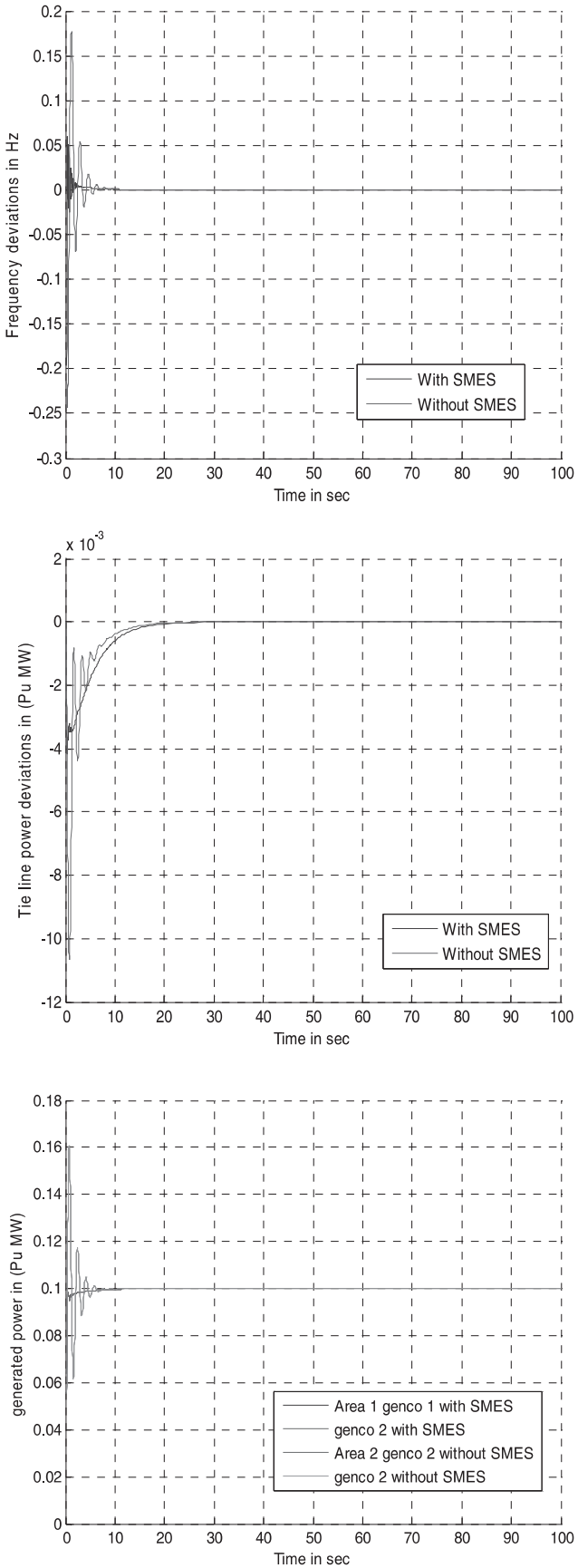

Fig. 5 Comparative dynamic responses with or without SMES

VI. Conclusion

A comprehensive mathematical model for the AGC of a bilateral two area interconnected thermal-thermal power system fitted with SMES unit in area 1 has been presented in this paper and ACE parameters are optimized for an appropriate performance index by using LQR optimization method. The system frequency and tie-line power oscillations due to small load disturbances were found to persist for a longer duration even with optimal gain settings of integral controllers. It has been shown that these oscillations can be effectively damped out with the use of a small capacity SMES unit in either of the areas following a step load disturbance. It has also been observed that the use of ACE for the control of SMES unit substantially reduces the peak deviations of frequencies and tie-power responses.

APPENDIX A

Nominal system parameters of the interconnected two area thermal- thermal system are:

(i) System data

$a_{12} = -1$,
$T_{12} = 0.545$,
$B_1 = 0.425$,
$B_2 = 0.425$,
$R_1 = R_2 = R_3 = R_4 = 0.4167$Hz/p.u. MW,
$K_{P1} = K_{P2} = 120$Hz/p.u. MW,
$T_{P1} = T_{P2} = 20$s,
$T_{g1} = T_{g2} = T_{g3} = T_{g4} = 0.08$s,
$T_{t1} = T_{t2} = T_{t3} = T_{t4} = 0.3$s,
$apf_1 = apf_2 = apf_3 = apf_4 = 0.5$

(ii) SMES data

L = 2.65 H
$T_{DC} = 0.03$s
$K_{SMES} = 100$kv/unit MW
$K_{id} = 0.2$kv/kA
$I_{do} = 4.5$kA

REFERENCES

[1] Ibraheem, Kumar Prabhat, Kothari DP. Recent philosophies of automatic generation control strategies in power systems. IEEE transaction Power System.

[2] Ise T, Mitani Y, Tsuji K. Simultaneous active and reactive power control of superconducting magnetic energy storage to improve power system dynamic.

[3] Mitani Y, Tisuji K, Murakami Y. Application of superconducting magnetic energy storage to improve power system dynamic performance. IEEE Transaction Power System 1988.

[4] Tripathy SC, Balasubramania R, Chanramohanan Nair PS. Effect of Superconducting magnetic energy storage on automatic generation control considering governor dead band and boiler dynamics. IEEE Transanction Power System 1992.

[5] Tripathy SC, Balasubramania R, Chanramohanan Nair PS. Adaptive automatic generation control with superconducting magnetic energy storage in power system. IEEE Trans Energy 1992.

[6] Tripathy SC, Chanramohanan Nair PS. Automatic generation control with superconducting magnetic energy storage in power system. Electric Machines Power System 1994.

[7] Tripathy SC, Balasubramania R, Chanramohanan Nair PS. Effect of superconducting magnetic energy storage on automatic generation control considering governor dead band and boiler dynamics. IEEE Transanction Power System 1992.

[8] Mairaj uddin Mufti, Shameem Ahmad Lone, Sheikh Javed Iqbal, Imran Mushtaq: "Improved Load Frequency Control with Superconducting Magnetic Energy Storage in Interconnected Power System", IEEETransaction, 2007.

[9] Rajesh Joseph Abraham, D. Das *, Amit Patra. Automatic generation control of an interconnected hydrothermal power system considering superconducting magnetic energy storage in Electrical Power and Energy Systems 29 (2007) 571–579.

[10] Hadi Saadat, "Power System Analysis", McGraw Hill.

[11] I.J.Nagrath and D.P.Kothari, "Modern Power System Analysis", Tata McGraw Hill.